Experimental study on the influence of different thermal insulation materials on the fire dynamics in a reduced-scale enclosure

Leisted, Rolff Ripke; Sørensen, Martin X.; Jomaas, Grunde

Published in:
Fire Safety Journal

Link to article, DOI:
10.1016/j.firesaf.2017.09.004

Publication date:
2017

Document Version
Peer reviewed version

EXPERIMENTAL STUDY ON THE INFLUENCE OF DIFFERENT THERMAL INSULATION MATERIALS ON THE FIRE DYNAMICS IN A REDUCED-SCALE ENCLOSURE

Rolff Ripke Leisted[1*], Martin X. Sørensen[1,2] and Grunde Jomaas[1,3]

[1] Department of Civil Engineering, Technical University of Denmark, DK-2800 Kgs. Lyngby, Denmark
[2] now at If P&C Insurance, DK-2650 Hvidovre, Denmark
[3] BRE Centre for Fire Safety Engineering, Institute of Infrastructure and Environment, School of Engineering, University of Edinburgh, Edinburgh, UK

ABSTRACT

Four scaled (1:5) fire experiments with two identically classified types of commercially available sandwich panels incorporating either stone wool (SW) or polyisocyanurate (PIR) foam as cores were conducted using a modified version of the ISO 13784-1 (Reaction to fire tests for sandwich panel building systems — Part 1: Small room test) standard. This was to assess the suitability of scaled experiments for assessing sandwich panel fire behavior. In the modified version of the test standard (scaled and full experiments), the fire severity was increased to simulate fires that could occur in commercial premises. This was achieved by prolonging and doubling the heat release rate output of the gas burner at the end of the experiments. Furthermore, non-structural damages such as screw-hole damages were applied to the enclosures to reflect real life observations.

The results showed differences in the fire behavior, depending on whether the enclosures were constructed of panels filled with SW or PIR insulation material. The mass losses of the insulation materials showed significant contribution from the PIR cores, regardless of fire load and the non-structural damage.

The qualitative behavior with respect to the “flashover” failure criterion, as stated in the ISO 13784-1, was successfully obtained in all of the scaled experiments. As such, the scaled experiments mimicked the behavior of the full scale SW experiments to a satisfactory degree. However, the PIR compartments failed considerably earlier in the full scale tests than in the scaled experiments. Therefore, it can be concluded that when the energy contribution from the core material remained negligible compared to the gas burner, the measured parameters matched quite well. Therefore, if the insulating core material does not dominate the fire dynamics of the compartment and the energy from the gas burner dictates the fire scenario then the scaled set-up will predict the temperature in the full scale compartment. Based on this and with further development with respect to, especially, time, this kind of scaled experiments could be a valuable testing method for assessment of the behavior of sandwich panel, and therefore merit further studies and eventually increased use.

*Corresponding author: rrle@byg.dtu.dk

1. INTRODUCTION

Pre-fabricated sandwich panels, typically composing of 0.5-1.0 mm thick steel sheets bonded on each side of a core of insulation material, are increasingly popular as wall and ceiling materials in commercial premises [1], [2]. Sandwich panels are often used to replace brick, stone or concrete in structures such as factories and warehouses, and are widely used for construction of cold storage rooms or freezer facilities, and, as walls in general, as they allow rapid construction and provide excellent thermal insulation. Another reason for their popularity has to do with the increasing demands to meet carbon emission targets, which is important and required even in buildings where the risk of fire can be high [3]. Typically, the panels are ranging from 1 m to 1.2 m widths with lengths ranging from 2.5 m to 13 m, and they have thicknesses between 40 mm and 230 mm. The panels may be filled with polymeric foam (polyurethane, polyisocyanurate, phenolic or polystyrene) or wools (glass mineral or stone). Frequently, the panels are designed to interlock for ease of construction [2].

The combination of steel sheets on the outer faces and mechanical interlocks are not always sufficient to isolate the insulation materials from becoming involved during fires. In these cases, the panels can become involved in the fire, and large fires where sandwich panels formed the enclosure have occurred, each resulting in losses of several hundred million Euros [4], [5]. These losses were observed despite the fact that the sandwich panels used were classified according to known standards [6], [7], [8]. It is important to point out that this is not necessarily a deficiency of the classification methods, but rather a result of the discrepancy between the test-standard fire scenarios and the actual fire scenarios that the panels experienced where they were installed. Furthermore, the insurance records were just on compartment fires. However, sandwich panels are also being used as external façades but are outside the scope of this paper as they are tested differently.

The current series of scaled experiments were conducted using panels with two different insulation materials that both had been approved by internationally recognized standards. The cores were of polyisocyanurate (PIR) and stone wool (SW) with conductivities at ambient of 0.021 W/m·K and 0.038 W/m·K and a core density of 30 kg/m^3 and 120 kg/m^3, respectively. Besides their internal use these two sandwich panels are also approved for use as external façades. However, the focus of this paper is not external (vertical or horizontal) flame spread. These experiments were carried out in a 1:5 scale of the full scale experiments, which were conducted in a similar fashion [9].

The ISO 13784-1 (Reaction to Fire Tests for Sandwich Panel Building Systems — Part 1: Small Room Test) [10] test standard, which formed the basis for these scaled experiments, prescribes a fire intensity of 100 kW for the first 10 minutes followed by 300 kW for the next 10 minutes and ends with a 10 minute observation period, for a total test duration of 30 minutes, as presented in Fig. 6 for the first 20 minutes, and similar to the third compartment fire test in the FM 4880. The failure criterion in the ISO 13784-1 is met when the total heat

release rate (HRR) from the ignition source and product exceeds 1000 kW for more than 10 seconds. Herein, however, the fire scenario itself was modified to be of a greater challenge to the panels, as compartment fires are complex and can differs from the test conditions described in the test standard. This modification entailed increasing the fire intensity and the fire load by doubling the heat release rate of the gas burner after 20 minutes and by allowing the experiments to run for longer than the 30 minutes prescribed in the ISO test standard [10]. The fire scenario was designed to be as challenging as possible while staying within the paradigm of the ISO 13874-1 and without changing the fire dynamics beyond that of an ordinary compartment fire. 600 kW was chosen to be large enough to challenge the panels, as insurance record indicated that fires causing large claims were both more intense and lasted longer than the standard test duration. Additionally, the panels were subjected to simulated damages such as unsealed screw holes piercing the protective inner metal sheet. These preconditions in the scaled experiment were also applied to the previously conducted full scale experiments [9], with the main objective being recreation of similar results across the two set-ups. The purpose of conducting the experiments with damaged panels was to establish what, if any, impact compromising the panel would have on the compartment fire. For this reason, the mass loss of the insulation material was monitored by placing the entire rig on a scale during the experiments.

Using scaling correlations, the heat release rate provided by the gas burner was scaled, and so were the periods of time for each step. Carvel et al. [11] found that gaps will form in the joints of sandwich panels exposed to fire, especially when directly affected by the fire. As a result of these gaps, a rapid heat discharge took place, and the panels were observed to contribute to the fire growth. Because scaled experiments are unable to predict the behavior of the joints and mechanical fastenings during a fire with great accuracy, certain concerns have been raised with respect to using this method for assessing sandwich panel fire performance [12], [13]. Herein, the behavior and not the failure mode of the sandwich itself was not the main focus. The scaling methodology was carried out in order to assess whether or not the scaled experiments could be used to understand how the choice of insulation core materials affected the overall fire dynamics. Also, the impact of exposed core surfaces with respect to fire growth was of interest.

2. EXPERIMENTAL SETUP

Fire is complex, it depends on both physical and chemical processes and is not possible to get a perfect or complete scaling across all scales for all parameters. Therefore, similar fire dynamics must be achieved through appropriate partial scaling [14]. Partial scaling is achieved by determining which aspects of the fire behavior that are of most importance. As this is dependent on the scenario and the research focus, there is not a universal way to carry out experiments of this nature. The applied scaling correlations of the heat release rates are based on the applications of Froude scaling, which is a widely used application technique

within enclosed fire research. Herein, the fire load was provided by a gas burner, with no additional fuel load in form of wooden cribs etc., and the partial scaling of its HRRs became more reliable as the gas supply was perfectly monitored and controlled digitally with a flow meter. The applied scaling correlations of the heat release rates are based on the applications of Froude scaling, which is a widely used application technique within enclosed fire research. In the work of Carey on scale modeling of static fires [15], the scaling of the HRR is presented as a dimensionless value and is concluded to be useful for all fuels to match the scaled HRR to the full scale HRR. The same was concluded by Wang et al. in their work with scale modeling of compartment fires for structural fire testing [16]. Furthermore, Quintiere found that results from model scale testing fitted the large scale data well [17].

An entirely new experimental rig the sandwich panels was developed. The size of the rig was scaled geometrically as 1:5 relative to the dimensions of the room described in the ISO 13784-1. The internal dimensions of the full scale test room are specified as 3.60 m x 2.40 m x 2.40 m ± 0.05 m (L x W x H), with the door opening dimensions of 0.8 m x 2.0 m (W x H) and the internal dimensions of the scaled test rooms were therefore 0.72 m x 0.48 m x 0.48 m ± 0.01 m (L x W x H), with the door opening dimensions of 0.16 x 0.40 m (W x H). Sandwich panels constituted the walls and ceiling and formed the room enclosure, which can be seen in the schematic in Fig. 1. The floor consisted of a 5 cm cured ceramic board, which is also in accordance to the test standard requirements (an inert floor covering is prescribed).

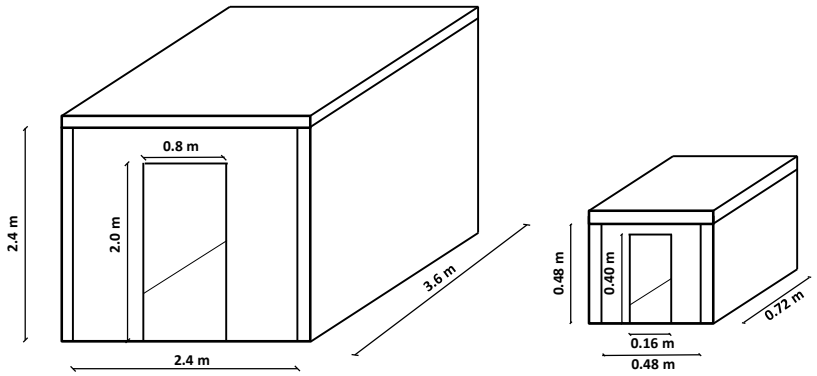

Fig. 1: Internal geometry of experimental sandwich panel enclosures. *To the left:* Full scale geometry. *To the right:* Scaled geometry (1:5).

The panels were mounted so the ceiling panel rested on the walls and the end panels were wedged in between the two panels for the longer sides. As panels in their end-use often have flashings along edges it was also done herein by fastening various 2 mm thick flashings with 4 cm long and 4 mm thick both in stainless steel. L-profiles measuring 2.5 cm by 2.5 cm were fastened internally every 0.12 m along all ceiling and wall corners. Externally, 15 cm by 5 cm L-profiles were fastened along the ceiling and walls with 15 cm intervals and along the door frame the exposed core was protected by 10 cm by 2.5 cm U-profiles fastened every 8 cm. The fuel source was a newly developed gas burner. This sandbox burner was geometrically scaled with a similar scaling ratio of 1:5. This ratio applies to the lengths of the surface opening of the burner as well as the distance from the top of the burner to the floor. The burner prescribed in ISO 13784-1, and used in full scale testing, measures 170 mm x 170 mm

x 200 mm (L x W x H) while the scaled burner was designed to measure 34 mm x 34 mm x 40 mm (L x W x H). Furthermore, to ensure that an even gas flow was achieved over the entire opening area of the burner the internal height of the container was designed to be 100 mm, rather than the necessary 40 mm, as seen in Fig. 2. This choice of design was also made to allow the burner to be fitted through the inert floor board in the rig, and thereby allowing the gas inlet tube to be connected from beneath without compromising the integrity of a wall. As the distribution of gas across the burner opening was ensured by the porous medium, the increased burner length is believed to be of negligible influence on the flow. The main body of the sandbox burner consisted of a square tube cylinder on which a bottom stainless steel plate butt was welded onto. The plate was 3 mm thick. A ¼ inch (0.64 mm) outer diameter Swagelok tube fitting was threaded through the bottom plate on which the gas inlet tube was connected. The 2 mm thick and 15 mm wide horizontal welded plate around the main body of the burner ensured support and sealed the hole during experiments. The bottom 64 mm of the cylinder was filled with fine gravel (4-8 mm) and the top 33 mm was filled with very fine gravel (2-3 mm) separated by a brass wire gauze with a mesh size of 1.8 mm. The upper layer of gravel was in level with the upper edge of the burner. The burner was situated in a corner opposite the wall with the door opening. At no time was additional fuel added in the compartments in these scaled experiments and the terminologies of *fuel controlled and ventilation controlled* are therefore favored instead of *flashover*.

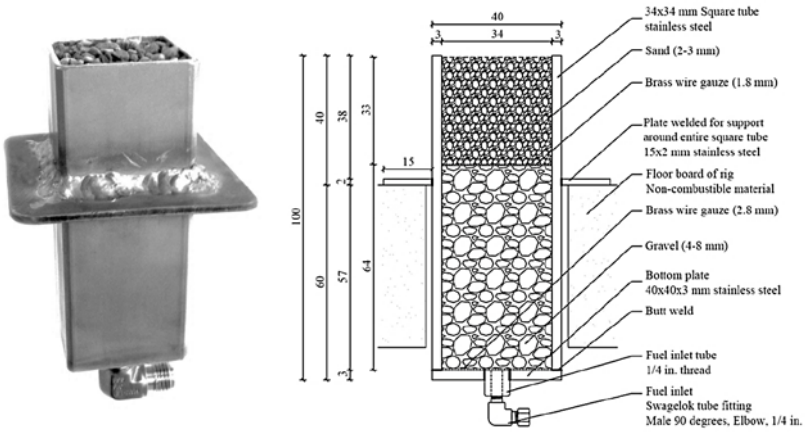

Fig. 2: *To the left:* The designed sandbox burner. *To the right:* The conceptual design of the burner. All dimensions are in mm, unless specified otherwise.

2.1. METHODOLOGY

The volumetric flow rate of the gaseous fuel was adjusted based on maintaining the Froude number identical across the two scales which implies the non-dimensional heat release rate, $\dot{Q}^*$ remains the same across the two scales. The scaling correlation of the heat release rate is given by Eq. 1 [16], [18], [19], [20],

$$\frac{\dot{Q}_M}{\dot{Q}_F} = (S)^{5/2} \quad (1)$$

Where $\dot{Q}_M$ is the scaled heat release rate of the model, $\dot{Q}_F$ is the heat release rate used for the full scale experiments and S is the scaled ratio and l_M/l_F, is the model length divided by the full scale length. This ensures that the flame temperature will be identical along their relative vertical axis. The single gas burner provides the relative same convective heat flow into the compartments by maintaining the relationship between the inertia forces of the gas and the graviton forces. Convection was prioritized as the governing mode of heat transfer with this scaling. The relationship between convective heat transfer and temperature is linear, whereas the radiative heat transfer increases with temperature to the fourth power. With the prioritization of convective heat transfer, the radiation is assumed to be negligible, which will be the case for lower temperatures. However, as the fire dynamics in the compartment change from a well-ventilated to an under-ventilated fire, the combustion efficiency will decrease and the reaction will favor a higher production of CO and soot which will directly influence the smoke layer. This ultimately means that the scaling relationship, which relies on the burner being the dominant fire source, is less reliable if the fire dynamics of the compartment changes (i.e. becomes ventilation controlled). Therefore, the estimated HRR from the full compartment cannot be inversely calculated to equivalent full scale HRR, but remain an indicator of the growth and steady phase of the scaled compartment fire.

The compartment volume is defined as a Control Volume (CV) and the inner steel sheet of the sandwich panel are defined as the boundaries. Heat entering and heat leaving the CV is denoted Q̇ and $\dot{q}$, respectively. The heat transfer and equilibrium is based on Wang et al. [16] and expressed in Eq. 2.:

$$\dot{Q}_{in} = \dot{Q}_{burner} + \dot{Q}_{core} = \dot{q}_{vent} + \dot{q}_{out} + \dot{q}_{stored} = \dot{q}_{loss} \quad (2)$$

Where the total heat generated, $\dot{Q}_{in}$, consists of the heat input from the gas burner, $\dot{Q}_{burner}$, and the heat generated by the core, $\dot{Q}_{core}$. The heat losses, $\dot{q}_{loss}$, consist of the heat losses through the door opening, $\dot{q}_{vent}$, through the compartment walls, $\dot{q}_{wall}$ and the heat stored in the gas phase in the enclosure, $\dot{q}_{stored}$. A simplified schematic of the fire phenomenon in the compartment is shown in Fig. 3.

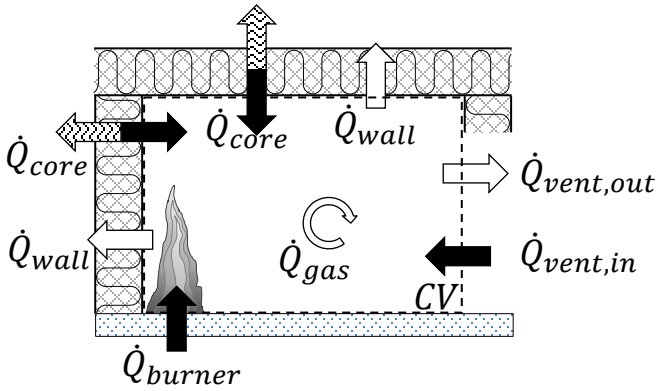

Fig. 3: Schematic of the Control Volume and the energy balance within the CV. Not to scale.

The net heat transferred to the internal walls which must balance out with the incident heat flux within the compartment, the radiation from the wall to the compartment, $\dot{q}_{rad}$, and the heat losses through the compartment walls, $\dot{q}_{cond}$, and the convective heat transfer between the wall and the compartment air, $\dot{q}_{conv}$, as seen in Eq. 3 and Fig. 4.

$$\dot{q}_{net} = \epsilon \dot{q}_{inc} + \dot{q}_{rad} + \dot{q}_{cond} + \dot{q}_{conv} \quad (3)$$

The difference between the gas phase temperature in the compartment and the temperature at the boundaries and the core temperature will determine the radiative, conductive and convective terms. The heat transfer interactions within the control volume (CV) will be determined by the energy input in terms of the HRR of the gas burner, which is being scaled. The heat transfer is controlled by the burner only as long as it is the dominant heat source in the compartment. However, the heat transfer and fire dynamics can also be controlled by the core if it contributes with enough additional heat, i.e. contributions beyond that of the burner, at which point it will dominate the changes in temperature. Therefore, the parameter of most interest is the unknown energy into the control volume, namely the energy contribution from the core materials, $\dot{Q}_{core}$.

In the full scale [9] and reduced scale the sandwich panels used were 100 mm thick. Thus, the size of the flame from the gas burner was larger in the full scale experiments relative to the thickness of the wall, than for the scaled experiments, as seen in Fig. 4. Furthermore, as the walls also are expected to absorb relatively more of the heat generated from the burner in the scaled experiments due to the thermal inertia remaining constant, the temperature development in the room was expected to be slower in the scaled experiments compared to the full scale experiments.

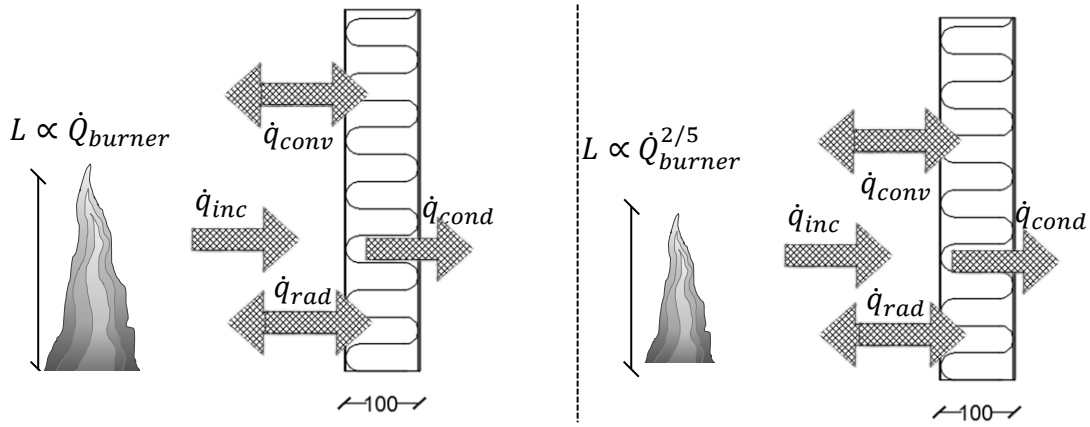

Fig. 4: Heat loss through the walls of the compartment. The wall thickness is given in mm. *To the left:* Full scale experiments. *To the right:* Scaled experiments.

In addition to scaling the heat release rate of the burner, the need for scaling the time parameter was apparent as the thickness of the walls remained the same. The scaling of the time parameter was based on Quintiere [19] and on Li and Hertzberg, who scaled internal wall temperatures in enclosure fires [18]. Their study concluded that these scaling correlations presented a good agreement between the results from the scaled experiments and the large scale experiments within a number of different focus areas, including the HRR and the time parameter. Li an Ingason successfully scaled a wood crib fire using Froude scaling and time scaling across a factor 4 between the scales [20]. The scaling correlation of the time parameter is given in Eq. 4 [18], [19], [20].

$$\frac{t_M}{t_F} = (S)^{\frac{1}{2}} \tag{4}$$

Where t_M is the scaled time period, t_F is the time period used for the full scale experiments and S is the scaled ratio and l_M/l_F, is the model length divided by the full scale length. The scaled HRRs and time parameters are presented in Table 1 for both the scaled and the full scale experiments.

Table 1: Scaled and full scale HRRs and time of corresponding burner stage.

Scaling ratio	Stage 1		Stage 2		Stage 3	
	HRR (kW)	t_1 (min)	HRR (kW)	t_2 (min)	HRR (kW)	t_3 (min)
1	100	10	300	20	600	30
1:5	1.8	4.5	5.4	8.9	10.7	13.4

Table 2: Experimental configurations of the scaled experiments.

Experiment number	Panel type	Propane burner output (min)			Non-structural damage applied. Screw-holes, on side panel adjacent to burner
		1.8 kW	5.4 kW	10.7 kW	
1	Stone wool	4.5	4.5	32.4	No
2	PIR	4.5	4.5	4.5	No
3	PIR	4.5	4.5	4.5	Yes
4	PIR	4.5	10.2	-	No

A total of four experiments were conducted, as summarized in Table 2 and measurements of temperature, mass loss and video graphic data were collected. The non-structural damage applied to the third experiment with PIR panels consisted of 5 x 10 mm diameter screw-holes and these were drilled through the inner metal sheeting and approximately 40 mm into the insulation material on the sidewall adjacent to the sandbox burner. The center hole was drilled 270 mm above the floor and 400 mm from the rear wall and four additional holes placed every 90 degrees and 127 mm radially from the center hole were likewise drilled, as seen in Fig. 5.

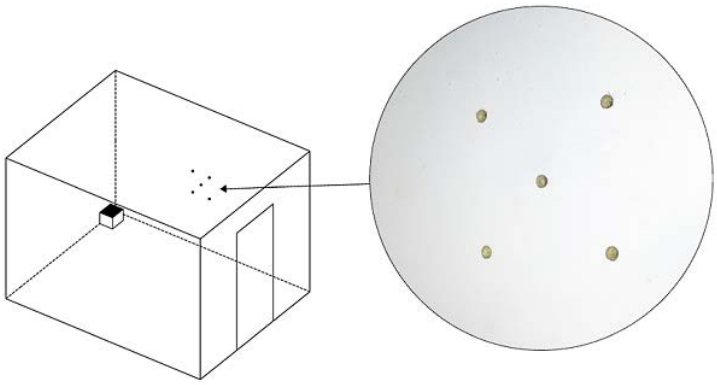

Fig. 5: Schematic of the inflicted screw-hole damage on the side panel adjacent to the burner. Not to scale.

The gas flow data was acquired through a mass flow meter. The flow of propane gas used to create the diffusion flame was controlled by regulating the mass flow meter and was increased in steps corresponding to the HRR stages shown in Fig. 6.

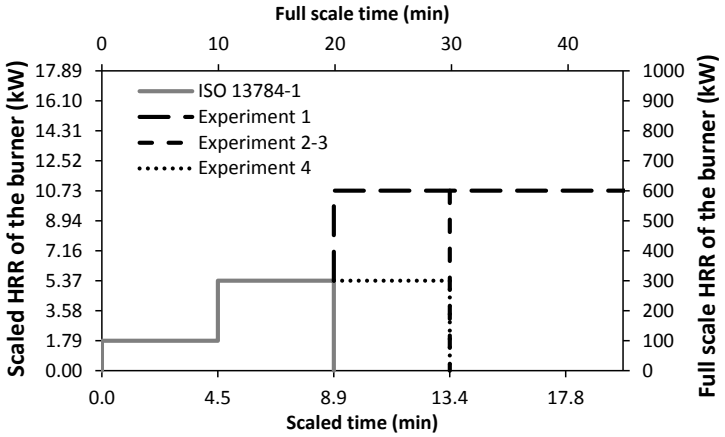

Fig. 6: The scaled HRR from the gas burner and corresponding full scale HRR for the four experiments

The entire rig was placed on a Sartorius EA35EDE-1 scale with a 60 kg capacity and 5 g (0.005 kg) readability. The data were digitally recorded every third second. An overview of the entire experimental setup is shown in Fig. 7.

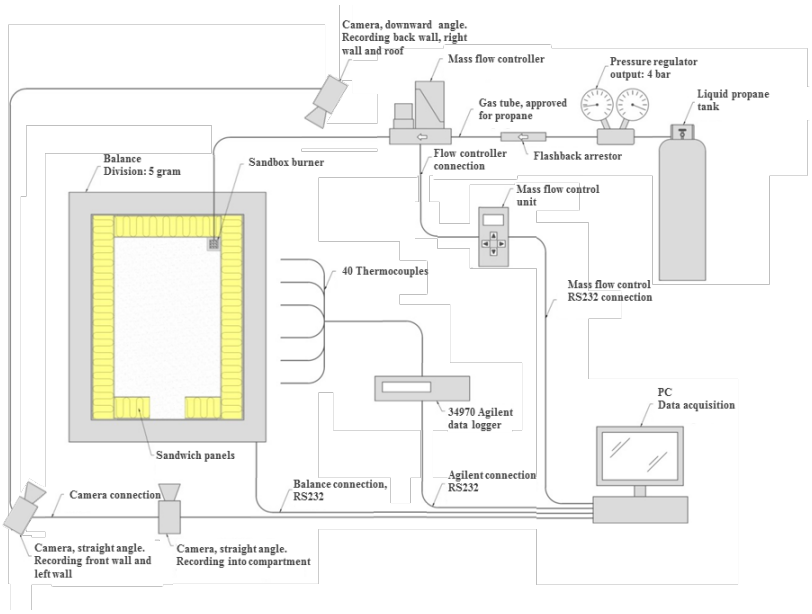

Fig. 7: Schematic of the scaled experimental set-up.

Temperature data were measured at multiple locations using type K mineral insulated thermocouple probes (1.5 mm in diameter and 250 mm long) in the sandwich panel walls and ceiling. The thermocouples were mounted from the outside of the compartment by drilling small holes from the outside of the panel and plugging in the thermocouple probe to the desired depth. Also, two type K thermocouple trees with 1.5 mm thick probes were located in the center of the compartment and in the door way. A 34970 Agilent Data Logger was used to log the temperature data with a sampling interval of 2.5 seconds. The thermocouples were located as shown in Fig. 8.

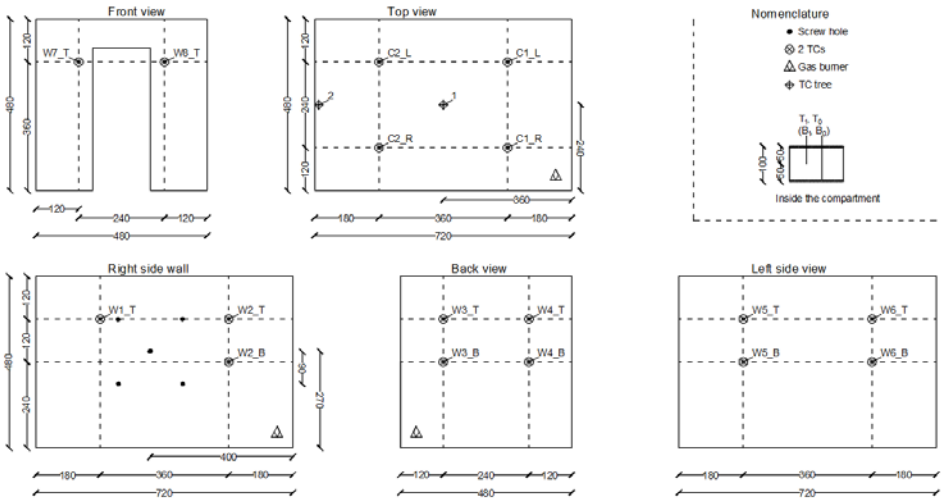

Fig. 8: Thermocouple locations in wall (W) and ceiling panels (C). All measurements are in mm.

The thermocouple tree in the center of the room, TC tree 1, measured the temperatures at distances of 50 mm, 150 mm, 250 mm and 350 mm from the ceiling. The thermocouple tree in the door opening, TC tree 2, measured the temperatures at distances of 70 mm and 170 mm from the upper door frame. Fig. 9 shows the configuration of the thermocouple trees.

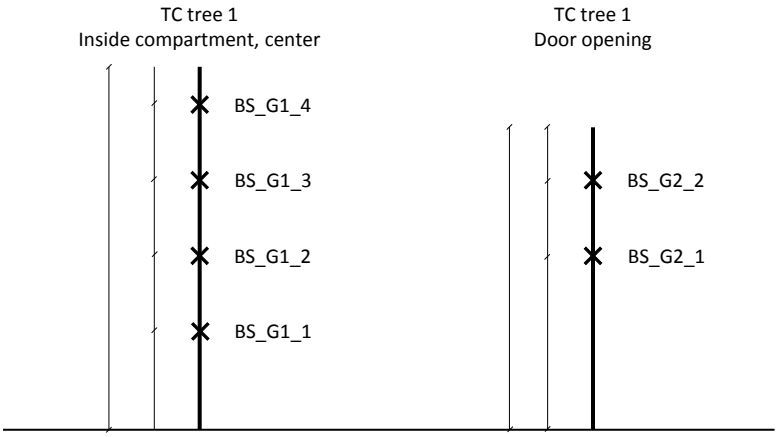

Fig. 9: Schematic of the thermocouple trees placed inside and in the doorway of the enclosure.

Three cameras were used to record the experiments for later analysis and review. One camera was placed behind the rig with a downward angle, recording the back and right-side wall as well as the ceiling panel of the compartment. The second camera was placed in front and perpendicular to the door opening, recording the compartment fire behavior through the door opening, as seen in Fig. 10. The third camera was placed opposite the first camera without an angle, recording the left-side and front of the compartment, as seen in Fig. 11a.

3. EXPERIMENTAL RESULTS

3.1. VISUAL AND PHOTOGRAPHIC OBSERVATIONS FOR ENCLOSURE WITH STONE WOOL PANELS

A sequence of photographs during the experiments with the stone wool enclosure is shown in Fig. 10. The 1.8 kW flame is shown in Fig. 10a. A few minutes after ignition, the coating of the sandwich panels in the close vicinity of the flame began to show signs of cracking. Fig. 10b shows the flame after the burner output was stepped up to 5.4 kW. Minor quantities of smoke were observed emanating through the door opening immediately after the burner output was stepped up to its final stage of 10.7 kW after 8.9 minutes, seen in Fig. 11a. The smoke subsided after another minute and became more transparent (less visible). 21 minutes after ignition, as seen in Fig. 10c, the enclosure had received 10.7 kW from the burner for around 12 minutes and a smoke layer was visible below the ceiling and pieces of burned coating were scattered on the floor in the enclosure. Small quantities of white smoke were observed emanating through the joints between the panels, shown for the ceiling panel after 21 minutes in Fig. 11b.

Fig. 10: The stone wool panel enclosure with scaled burner. *(a)* At ignition. *(b)* After 5 minutes. *(c)* After 21 minutes. *(d)* After 32 minutes.

Similarly to what was observed in the full scale stone wool experiments [9], the smoke was predominantly transparent, suggesting that the majority of the gases originated from the complete propane gas combustion with little contribution from the panels to the fire. The contribution at this stage was most likely from the adhesive used to bind the metal facings to the slab of stone wool and the coating. The gas supply was turned off after 42 minutes, at which point the compartment temperature had stabilized slightly below 600 °C for around 20 minutes, as seen in Fig. 14.

(a) (b) (c)

Fig. 11: Front and back view of the stone wool panel enclosure, (a) Front view after 9 minutes, (b) Back view after 21 minutes and (c) Front view after 32 minutes.

3.2. VISUAL AND PHOTOGRAPHIC OBSERVATIONS FOR ENCLOSURES WITH POLYISOCYANURATE PANELS

The fire development in the enclosure with undamaged PIR panels is shown in Fig. 12, and Fig. 12a shows the 1.8 kW flame 2 minutes after ignition. At this point, transparent white smoke had started to form a layer below the ceiling. 7 minutes after ignition (Fig. 12b) a thick smoke layer had formed, with dark and sooty effluents pouring out of the door opening, indicating that the PIR contributed to the fire. A rapid transition occurred where large quantities of smoke were produced and filled up the vast majority of the enclosure after 8.5 min, as seen in Fig. 12c. Additionally, unburned pyrolysis gases from the panels began pouring out under the panels along the sides as well as from the back of the enclosure, as seen in Fig. 13a, which was an indication of further decomposition of the PIR. The transition from a fuel to a ventilation controlled fire occurred between 8 min 15 s and 9 min 30 s, as determined by temperature measurements along the height of the door opening and inside the compartment, and observed visually (see Fig. 12c and Fig. 12d). Further development can be observed in Fig. 13b, where the burner had just been stepped up to 10.7 kW, and large flames had emerged outside the doorway. After 11 minutes, the flammable gases emanating on the external side of the back panel ignited, and after 13 minutes, as seen in Fig. 13c, all four external walls of the room were burning. Throughout all the experiments involving PIR panels, sounds of metal expanding and being distorted were heard.

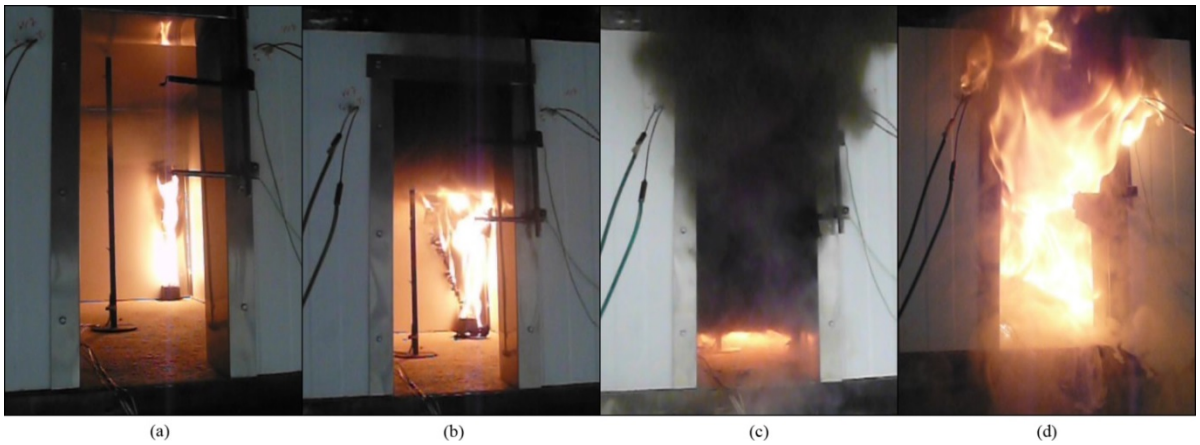

(a) (b) (c) (d)

Fig. 12: The PIR panel enclosure without damages, front view. *(a)* 2 minutes after ignition, *(b)* After 7 minutes, *(c)* After 8.5 minutes and *(d)* After 9 minutes.

After 8.5 minutes of experiment 3 (see Fig. 13), which was moments before the enclosure was rapidly filling with smoke, small flames were observed to emerge from the screw-holes drilled into the wall adjacent to the burner. Experiment 4 was carried out with a prolonged second burner stage instead of the third stage and no significant differences were qualitatively observed in terms of the fire development and over all fire dynamics. The visual observations made during these experiments were in line with those observed in the full scale experiments [21] with regards to the behavior of the compartment, lack of joint separation and external flaming emerging from the corner joints and joints between ceiling and wall elements.

Fig. 13: Front (top row) and back (bottom row) view of PIR experiment 2. (a) 8.5 minutes after ignition. (b) After 9 minutes. (c) After 13 minutes.

3.3. TEMPERATURE MEASUREMENTS

The weighted average temperatures measured in the upper gas layer (in the center of the compartment) are shown in Fig. 14. The data shows that there is quantitative agreement between the PIR and the stone wool for the first 4.5 minutes of the experiments, where the gas burner output was 1.8 kW. At 4.5 minutes, when the burner output was increased to 5.4 kW, the behavior of the two enclosures starts to diverge. The fire started to grow rapidly in the PIR panel enclosures, observed as the temperatures increased from 150 °C to 600 °C due to contributions from the PIR core, resulting in transitions into ventilation controlled fires in all the experiments near the 9 minute mark. The data shows that regardless of whether the gas output was increased to the final stage of 10.7 kW, as for experiments 2 and 3, or kept at the second stage of 5.4 kW, as for experiment 4, the development of temperature within the room was approximately the same. This is also in line with the visual observations made that the fire growth, which thus must be linked to the contribution from the PIR, started before the final stage of the heat release from the burner was initiated. In the full scale experiments [9], the transition to flashover occurred in the PIR enclosure with a wooden crib 11.5 minutes into the experiment. This is in line with previous experimental work done by Axelsson and Van

Hees [22], as they found that flashover occurred at 11.75 minutes when conducting experiments according to the ISO 13784-1 (although, their use of the term "*flashover*" here refers to the transition to a ventilation controlled fire, because no additional fuel in the compartment was present, as prescribed by the ISO test procedure).

The temperature profile in the stone wool enclosure seems to follow the shape of the heat release rate supplied by the gas burner, as seen in Fig. 6. However, unlike the full scale experiments, the temperature did not stabilize during the first steps of the burner, as the thermal inertia was not scaled and the thickness of the panels being identical in both the full scale and model scaled experiments. The much smaller flame size in the scaled experiments does seemingly not cause the same heat flux through the wall panels compared to the larger flame in the full scale experiments. This result in the panels were able to, relatively, absorb more of the heat in the room for a longer period of time in the scaled experiments. This lowered the rate at which the compartment temperature increased. The room temperature stabilizes when the heat transfer through the walls have reached steady state, which took relatively longer for the model scaled experiments, as seen in Fig. 14. After entering the third burner stage, the temperature in the top of the SW compartment stabilized after 20 minutes to just below 600 °C for the remainder of the experiment for both the model and full scale experiments, as seen in Fig. 14.

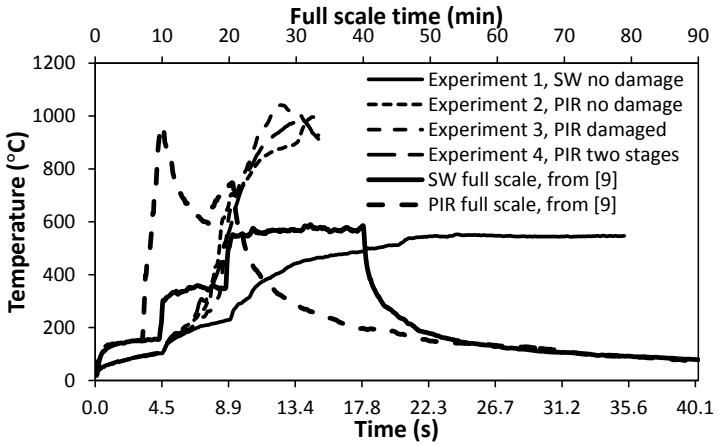

Fig. 14: The weighted average temperature of the upper layer (in the center of the enclosure) in the scaled experiments and data from literature [9].

The temperature of the gas leaving the compartment through the door opening was measured at a height of 33 cm from the floor, as seen in Fig. 9, while the corresponding full scale measurement location was at 160 cm (160 cm/5 = 32 cm). The temperature comparison between the SW experiments, as shown in Fig. 15, compare well in the upper layer of the door opening. However, the temperature in the two PIR experiments only show the same initial slope when their respective transitions to ventilation controlled phase occurred as well as similar peak temperatures, albeit at different times.

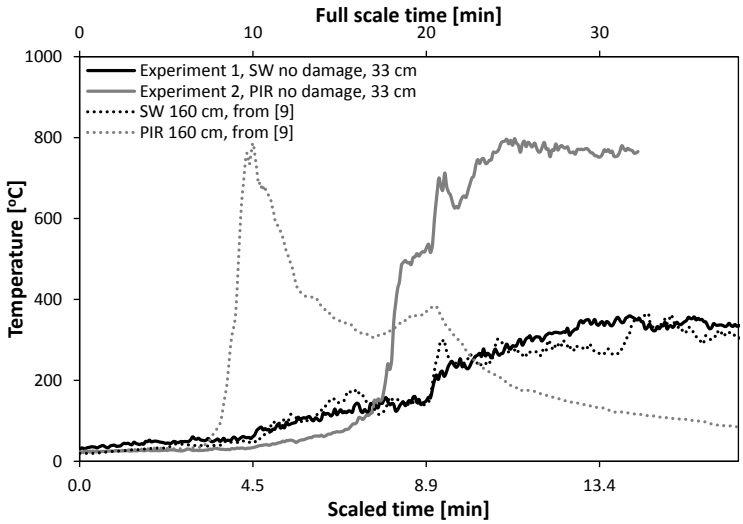

Fig. 15: The temperature of the gases leaving the compartment measured in the door opening.

Fig. 16 shows the temperature on the inside metal face of the wall panel adjacent to the burner, labeled W3 (see Fig. 8). The data shows reasonable agreement between the wall temperatures and the room temperatures at ceiling level during the first burner stage, as seen in Fig. 14. In the first stage, the PIR and SW enclosures absorb about the same amount of heat and have similar temperatures. However, the temperature shows that a possible thermal runaway takes place in the PIR panel after the second gas burner stage is initiated. Alternatively, this could be the coating burning locally. This indicates that the PIR is reacting and starts to contribute with additional heat to that from the burner, which would further accelerate the combustion rate and mass consumption of the PIR. For the first 7 minutes the measured temperature in the compartment was higher than the wall and thereafter the wall became warmer than the ceiling level of the compartment.

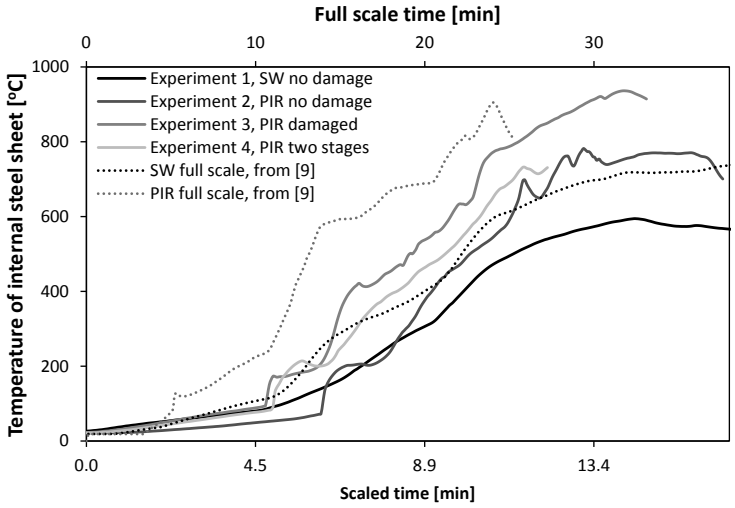

Fig. 16: The temperature measured on inner metal sheet in wall panel *W3* in scaled experiments 1 (SW) and 2 (PIR) along with two measurement points at the same relatively height from literature [9].

Fig. 17 shows the temperatures in the middle of the insulation core in the wall panel adjacent to the burner, labeled W3 (see Fig. 8). The panel temperature indicates that it took 12-13 minutes for the heat to penetrate and reach the middle of the PIR core, upon which the temperature increased rapidly.

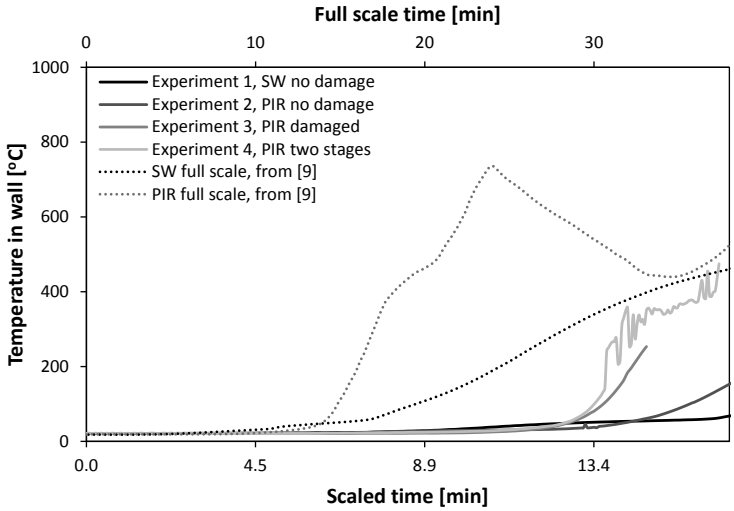

Fig. 17: The temperature in the middle of the insulation core in wall panels *W3* in the scaled experiments 1 (SW) and 2 (PIR) along with two measurement points at the same relatively height from literature [9].

A further examination of the temperature evolution in the middle of the panel cores, as seen in Fig. 17, reveals that there are similar temperature gradients between the scaled and full scale experiments [9], as seen in Fig. 18. The temperature gradient in the center of all the 6 cores remained negligible for the first 7 minutes of their respective experiments and both SW cores penetrated by the thermal heat wave had an initial peak after 10-12 min and a sudden increase again after 16 min before stabilizing. As the burner was increased prematurely in the full scale PIR experiment its corresponding gradient, seen in Fig. 18, has been offset those 3 minutes, to match the initiation of the second burner stage with the scaled experiment. The temperature gradients in the center of the PIR cores show an initial heat wave passing through the scaled core without a similar behavior in the full scale. The reason for the sudden increase not occurring in the full scale might be the shortened duration of the first burner stage. Nevertheless, after approximately 12 minutes of both the scaled and the full scale experiments, it was observed that the PIR core temperature started to increase. The temperature increase in the scaled experiment took place earlier than in the increase in the full scale experiments, but they were not as steep.

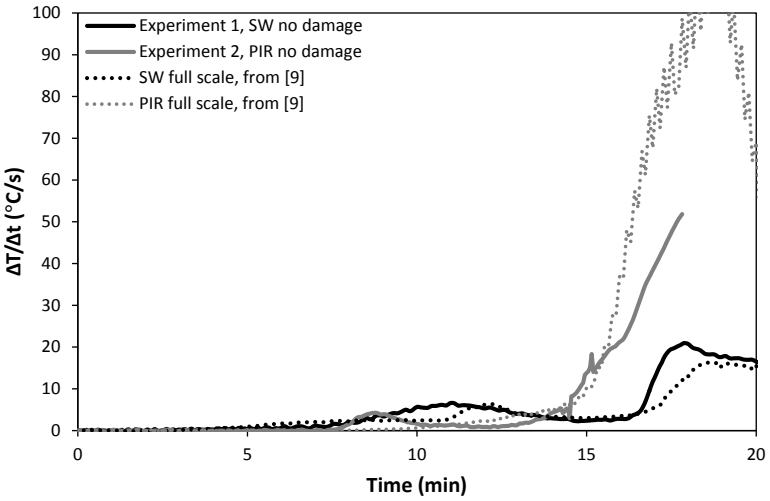

Fig. 18: The temperature gradient with respect to time measured in the middle of the insulation core in wall panel *W3* in the scaled experiments 1 (SW) and 2 (PIR) along with two measurement points at the same relatively height from literature [9].

3.4. MASS LOSS MEASUREMENTS

Fig. 19 shows the mass loss of core insulation materials during the experiments, calculated as the percentage of core mass from their respective initial mass as well as the raw mass loss in kg. The average initial mass of the PIR panel enclosures were 24.01 kg ± 0.02 kg and the initial mass of the stone wool enclosure was 37.04 kg. It is only the mass of the core in the panels that is included in the figure (i.e. the weight of the rig, steel facings and other equipment is excluded).

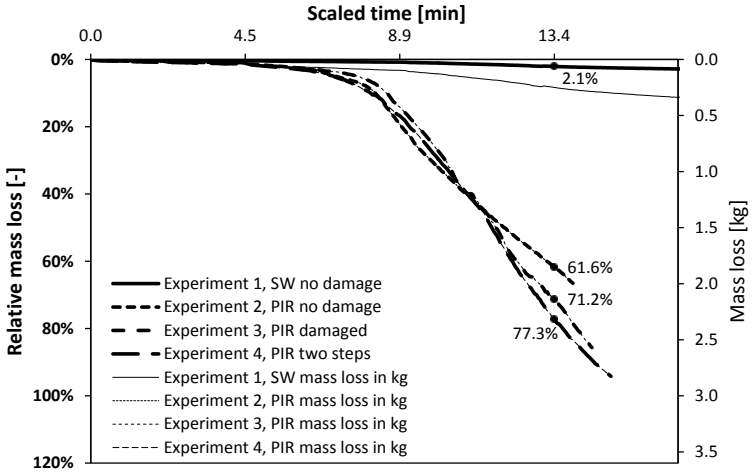

Fig. 19: Relative mass loss percentage of initial mass as well as total mass loss in kg. Mass loss in percent with bold on the left vertical axis and mass in kg on the right vertical axis.

The respective energy input from the burner in each of the three PIR experiments was sufficiently large to cause a significant mass loss starting at around 8 minutes. This indicates that the significance of whether or not the panels were damaged (as done herein) prior to

conducting the experiment was negligible. Likewise, the lower gas burner output during experiment 4 was of no significance, as the mass loss rate started to take off prior to the final burner stage. The heat release was generated by the sandbox burner and by combustion processes in the panels. As the heat release from the burner was constant within the individual stages of the experiments, the rapid increase in both the temperature and mass loss rate mid-stage were results of the contribution of extra heat released by the PIR as it started to pyrolyse.

The total mass loss of the stone wool panel enclosure, burning for 41.9 minutes, was 5.42% of its initial core weight and 2.05% after 13.4 minutes, which is consistent with the observations made during disassembly of the enclosure. The adhesive used to bind the metal sheet and the insulation core adds to approximately 1% of the total mass on the entire panel, according to the manufacturer specifications, and must have decomposed in order for the metal sheets to delaminate from the core. The mass loss of the core in the PIR panel enclosures, after burning for 13.4 minutes, varied from 61.6% to 77.3% depending on the experiment settings with experiment 4, with the prolonged second burner stage, losing the least, suggesting some influence from the HRR of gas burner in maintaining the intensity of the fire during the steady phase.

3.5. ESTIMATION OF TOTAL HEAT RELEASE RATE FROM THE PANELS

The three PIR compartments and the single SW compartment experimented on were exposed to identical thermal attacks by the gas burner during the first 8.9 minutes. The only difference with respect to the fuel load in the compartments was the difference in their respective core materials. Their respective heat release rates from the core, $\dot{Q}_{core}$, is estimated with Eq. 5

$$\dot{Q}_{core} = \dot{m}_c \cdot \chi \cdot \Delta H_c \quad (5)$$

Where $\dot{m}_c$ is the measured mass loss rate of the core, χ is the combustion efficiency and ΔH_c is the complete heat of combustion of the core. However, the combustion efficiency cannot be known as it is a function, of the instantaneous changes of the ventilation conditions in the compartment and is changing over time. The calculated HRR is therefore presented merely as a range. Based on another, unpublished, scaled compartment experiment the mean combustion efficiency was determined as 0.61 with deviations between 0.4 and 0.6 as its lower and upper limits, respectively. The estimated HRR based on mass loss rate marked with vertical deviation lines for the four experiments can be seen in Fig. 20.

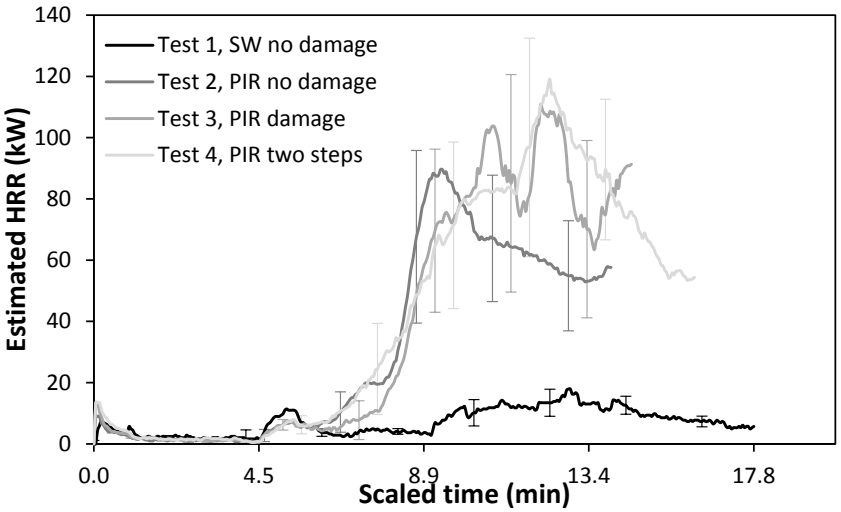

Fig. 20: The estimated heat release rate based on the mass loss rate of the panels.

The maximum mass loss rate for all the experiments occurred past the 8.9 minute marker, thus, for the PIR compartments during their ventilation controlled phase, and for the SW during the third burner input stage. The maximum mass loss rate measured was: 0.8 g/s, 6.6 g/s, 8.2 g/s and 8.8 g/s for experiment 1 to 4, respectively. For the PIR the complete heat of combustion, ΔH_c, is taken as 22.2 MJ/kg [23]. This calculates as an additional heat release rate at the end of the second burner stage as between approximately 53 kW and 78 kW added by the PIR panels to the overall system. This is between 10 times and 15 times the burner input for this stage. The complete heat of combustion for the SW core, being a Class-A building material [6], cannot be higher than 3 MJ/kg. However, the majority of the mass lost was assumed to be the polyurethane glue binding the SW slaps to the steel face and the organic binder in the SW core which has a complete heat of combustion of 24 MJ/kg [23]. The SW panels released between 7 kW and 18 kW throughout the duration of the experiment resulting in a HRR to burner output ratio spiking initially to 3.5 and, excluding the ramp ups of the burner, otherwise remaining below 1.5 throughout the 40 min duration of the experiment compared to the PIR panels that released up against 5 to 29 times the burner output past the second burner stage. These are all estimated values as the combustion efficiency had to be assumed. For the PIR panel experiments, transition into ventilation controlled conditions occurred before the initiation of the third and final burner stage at which point the combustion efficiency would rapidly change and be different from the extrapolated value. However, still within the range provided from the other experiment as it also transitioned into a ventilation controlled compartment fire.

The ratio of the total heat released by the insulating material that actually combusted inside and outside the compartment is unknown, but the potential of heat released is nevertheless increased significantly with a combustible insulation core as these results show. The conservative estimate with the combustion efficiency set to 0.4 indicate that in average at least 420% additional heat was generated during the first 13.4 minutes for the PIR experiments, of which the vast majority was released during the final burner stage with ratios reaching 4.2, 5.3 and 10.8, for experiment 2, 3 and 4, respectively. Thus, orders of magnitude

of additional potential heat were being released into the compartment, and surroundings, by the combustion of PIR compared to that of the propane from the gas burner. The ratio between the total energy released by the cores compared to the total heat released, as seen in Fig. 21, shows that the SW core released 60 %, 49 % and 52 % of the total energy for the three burner intervals, respectively. Experiment 2 with PIR core released 52 % of the total energy released during the first burner step and 77 % and 86 % of the second to last and last, respectively. Lower and upper error bars, as seen in Fig. 21, indicating the uncertainty associated with the combustion efficiency ranging from 0.4 to 0.8, respectively.

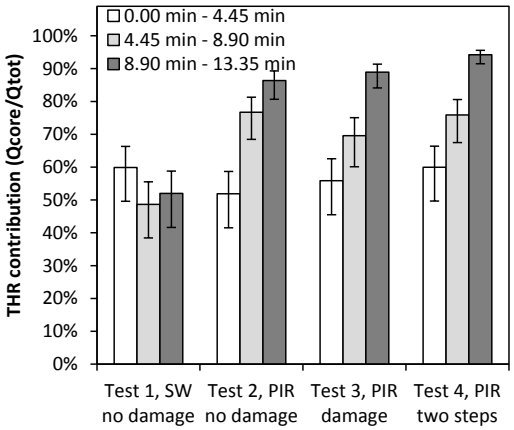

Fig. 21: The Total Heat Released by the core to the total heat released.

4. DISCUSSION

The direct comparison of the temperatures in the scaled with the full scale experiments [9] got complicated by the second burner step in the full scale PIR panel experiment being initiated earlier than planned (by mistake it was initiated after 7 min instead of after 10 min), as well as the third burner step being shortened, just 3.3 mins of duration. However, the core temperature evolved in similar ways as in the scaled experiments, as did the hot gases leaving through the doorway in the SW compartments. With similar heat transfer through the compartment boundaries and through the door opening between the scaled and full scale experiments the overall compartment fire dynamics is believed to be somewhat well mimicked in these scaled experiments. However, this is only the case for the SW panels, where the compartments did not change from fuel to ventilation controlled but eventually reached a steady state situation where the gas temperature in the compartments stabilized. The fire dynamics in the PIR compartments differed a great deal on many parameters when comparing the scaled with the full scale experiments. Some of the potential fuel stored in the combustible walls was released and dominated over the gas burner. The a priori scaling theories used proved insufficient in mimicking the full scale behavior to the same degree as for the SW scenario. However, some conformity is found between the room temperature profile at ceiling level in the center of the room for the PIR panel enclosures in full scale [9] and the scaled set-up, as the temperature was around 130-150 °C when the burner was stepped up to 5.4 kW (300 kW for full scale). The temperature in the compartments increased

at a slower rate than in the full scale experiments [9] indicating that with this scaling configuration that the burner duration is not sufficient to mimic full the scale behavior perfectly. This could also be because, relatively speaking, more heat was being absorbed by the panels compared to the full scale. The influence of the joints between wall panels was not studied. The core along the joints is less protected than any core behind the steel and the lack of joints could potentially have influenced the fire dynamics and compartment temperature in unforeseen ways. However, as the burners across both scales were placed in the corner of the compartments near wall-to-wall and wall-to-ceiling joints the burner would influence them in a similar manner. Furthermore, as the hot upper gas layer is in contact with the ceiling and with all the wall-ceiling connections the effect of joints are not expected to play a significant role in the fire growth as the flow path for the pyrolysis gases was already short.

Large quantities of dark and sooty smoke was observed for several minutes prior to the ventilation controlled transition, which is coherent with the mass loss curves, showing significant mass loss starting from around 8 minutes. A transition to ventilation controlled conditions did not occur in the SW panel enclosures and the maximum weighted smoke layer temperature obtained in the compartment was slightly below 600 °C, which is similar to what was observed in the full scale experiment [9]. However, this can in some if not most cases be enough to cause a compartment to flashover [24] if the compartment contains other potential fuel sources (i.e. television, sofa, chairs, and stored goods) which is likely.

For both the PIR and SW experiments, there is an inconsistency between the scaled and the full scale [9] experiments regarding the time it took for the room temperatures to stabilize during each of their respective burner stages. This could be attributed to the thermal inertia and thickness of the compartment boundaries which were not scaled unlike the duration of the burner steps which were. A more thorough analysis on the differences in scaling compartment fires is too elaborate to be included herein, as it is a paper in progress of its own.

5. CONCLUSION

Scaled fire experiments with two types of insulation materials (stone wool and polyisocyanurate) were conducted using a modified version of the ISO 13784-1 (Reaction to fire tests for sandwich panels building systems – Part 1: Small room test) fire test. This was in order to evaluate the reproducibility of large scale fire test in a 1:5 scale set-up with the aim to compare and replicate the fire dynamics and possible failure criteria as well as to compare the performance of sandwich panel elements with identical international and insurance classifications.

The overall fire behavior in the experiment with the stone wool panels differed significantly from the behavior observed in the three experiments with the PIR panels. Throughout the first burner stage, however, the compartment temperature, mass loss and internal- and in-debt wall

temperatures all remained identical with only minor insignificant differences. During the second burning stage, the compartment temperature increased and as the PIR core material eventually reached its pyrolysis temperature differences in the fire development started to arise for the two sandwich panel types. A continuous release of pyrolysis gases from the PIR panels was observed, both in the scaled and the full scale experiments, when the compartment temperature reached approximately 140 °C. The subsequent ignition of these gases caused a change in the ventilation conditions inside the compartment. In the SW experiments, no ignition of the core material was observed, and the compartment temperature remained below the pyrolysis temperature of the core of the sandwich panel throughout the experiments.

The qualitative behavior with respect to the “flashover” failure criterion, as stated in the ISO 13784-1, was successfully obtained in all of the scaled experiments. The PIR compartment transitioned into ventilation controlled fires even before the modified burner stage was applied. The stone wool compartment absorbed the heat from the burner in similar manners for the scaled and full scale experiments and reached a steady state situation where the compartment temperature stabilized. The results of the scaled experiments showed a clear difference in fire development depending on the choice of insulation material. During the first step, the two materials insulated similarly, as indicated by the matching compartment temperatures. However, the scaled PIR experiments started to fail shortly after the second burner stage was initiated, as indicated by mass loss data, temperature data, as well as visual observations and video recordings. The maximum temperatures in the PIR enclosures were somewhat similar (around 1000 °C), but they occurred at different points in time (at the beginning of the second burner stage for the full scale experiments and at the middle of the third burner stage for the scaled experiments).

During the stone wool experiment, slight buckling of the metal sheeting occurred, and it was concentrated around the ignition source. The integrity of the joint located behind the burner was intact, and was of no significance to the development of the fire. Observations made during disassembly of the SW enclosure indicates that most of the polyurethane adhesive used to bond the metal sheet to the insulation core had been incinerated, as the metal sheets came apart from the stone wool slaps with little effort. The inflicted screw-hole damage showed negligible contribution to the fire, based on the analysis of mass loss data.

The sandwich panel with non-combustible faces and filled with combustible insulation did not provide an effective fire barrier and failed to provide the needed fire protection to withstand these fire scenarios. The mass loss of the combustible insulation material showed significant contribution from the core material (PIR), regardless of the fire scenario and non-structural damage. The panels with a stone wool (SW) core only produced a small amount of combustible gases, and therefore no change in the ventilation conditions was observed. As a result, it could be concluded that these panels passed the tests. From a fire safety perspective the sandwich panels with a core of SW thus performed better than the panels with a core of PIR for the current series of experiments. The non-structural damages to the panels exposing the core material did not change the fire development. Therefore, the change in ventilation conditions and the failure in the experiments cannot be attributed to the small areas of unexposed core. The released pyrolysis gases from the core need oxygen to accelerate the fire

growth and influence the compartment fire dynamics. As the temperature in the compartment increase and causes the released pyrolysis gases to expand, it is the delamination of the core from the steel faces that enables its transport into the compartment and delamination will be the dominant mode of failure. The delamination and generation of pyrolysates are what causes the panels to fail and both are controlled by the temperature thus making the scaling of the temperature essential.

Mixed observation were made with respect to the scaling of time, on one side the gas leaving the compartment through the doorway for the SW compartments matched quite well, whereas the thermal penetration time did not. However, it is believed the scaling of time should not have been used as the compartment temperature did not increase equally fast across the two scales and allowing for longer burner stages in the scaled experiments would increase the smoke layer temperature. Furthermore, the role of panel joints in small scale is not fully understood and should be resolved.

The scaled experiments mimicked the behavior of the full scale SW experiments to a satisfactory degree and this kind of experiments merit further studies and increased use. As the energy contribution from the core material remained negligible compared to the gas burner the measured parameters matched quite well. Therefore, if the insulating core material does not dominate the fire dynamics of the compartment and the energy from the gas burner dictate the fire scenario then a scaled set-up will predict the temperature in the full scale compartment. Based on this and with further development with respect to, especially, time, this could turn out to be a feasible testing method to assess the behavior of sandwich panel also under other fire scenarios.

ACKNOWLEDGEMENTS

The authors would like to thank If P&C Insurance, who supported the experiment by providing the sandwich panels and through direct financial support that enabled the construction of the new rig. In addition, the discussions with Ken Henningson, Anne Sønderskov-Nielsen and Phil Preston throughout the project are highly appreciated. Also, Jens Martin Dandanell at the Technical University of Denmark is thanked for his assistance with the construction of the scaled rig.

Finally, we appreciate the fruitful discussions we had with Morten Valkvist, at the time at NIRAS A/S, now at the Copenhagen Fire Brigade, about the scaling laws.

If P&C Insurance had no involvement in analyzing, interpreting, writing or submitting this article for publication.

BIBLIOGRAPHY

[1] K. Dedecker, J. Deschaght and R. Kumar, "Sandwich Panels - Supporting Growth with an Established and Proven Technology," PU Tech, Huntsman Polyurethanes, Belgium, 2008.

[2] J. M. Davies, "Lightweight Sandwich Construction," Published on behalf of CIB Working Commission by Blackwell Science Ltd., 2001.

[3] B. Messerschmidt, "Green Choices," *Fire Risk Management,* pp. 41-43, 2012.

[4] A. Rosenbom, "After the fire," *If's Risk Management Journal,* no. 2, p. 6, 2013, https://www.if-insurance.com/web/industrial/sitecollectiondocuments/risk%20consulting/riskconsulting02_13.pdf [accessed: 20/07/2017].

[5] S. Birt and T. Day, "Technical Briefing: Fire Performance of Sandwich Panel Systems," Association of British Insurers, 2003, http://www.bre.co.uk/filelibrary/rpts/sandwich/ABIsandwichPanels.pdf [Accessed 28/07/2017].

[6] *ISO 13501-1 + A1-2009, Fire classification of construction products and building elements - Part 1: Classification using data from reaction tests,* 2009.

[7] FM Global, *Approval Standard 4880 for fire performance.*

[8] *EN 13823:2010, The Single Burning Item Test,* 2010.

[9] M. X. Sørensen, J. M. Hidalgo, M. McLaggan, R. J. Crewe, S. Molyneux, A. Sønderskov, G. Jomaas, S. Welch, J. L. Torero, R. T. Hull and A. A. Stec, "Fire performance of sandwich panels in a modiefied ISO room test," *Materiały Budowlane,* no. 10, pp. 58-61, 2014.

[10] *ISO 13784-1:2002, Reaction to Fire Tests for Sandwich Panel Building Systems - Part 1: Small Room Test,* 2002.

[11] R. O. Carvel, J. L. Torero and D. D. Drysdale, *The Behavior of Sandwich Panels in Fire,* Institute for Infrastructure and the Environment: University of Edinburgh, 2002.

[12] P. van Hees and P. Johansson, "The need for full-scale testing of sanwich panels - comparison of full scale test and intermediate scale tests," *Interflam,* pp. 495-503,

2001.

[13] P. van Hees, "Only large-scale tests can properly evaluate the fire behavior of sanwich panels," *Brandposten,* no. 33, Published by SP, 2005.

[14] L. K. McCarthy, J. G. Quintiere, L. S. Reeves and A. J. Wolfe, "Application of Scale Fire Modeling," *Emerging Trends Newsletter,* no. 75, 2012.

[15] A. C. Carey, *MSc thesis: Scale Modeling of Static Fires in Complex Geometry for Forensic Fire Applications,* University of Maryland: Department of Fire Protection Engineering, 2010.

[16] M. Wang, J. Perricone, P. C. Chang and J. G. Quintiere, "Scale Modeling of Compartment Fires for Structural Fire Testing," *Journal of Fire Protection Engineering,* vol. 18, pp. 223-240, 2008.

[17] J. G. Quintiere, "Scaling Applications in Fire Research," *Fire Safety Journal,* no. 15, pp. 3-29, 1989.

[18] Y. Z. Li and T. Hertzberg, "Scaling of Internal Wall Temperatures in Enclosed Fires," *Fire Technology,* vol. 12 SP Report, 2013.

[19] J. G. Quintiere, Fundamentals of Fire Phenomena, John Wiley & Sons, Inc, 2006.

[20] Y. Z. Li and H. Ingason, "Scaling of wood pallet fires," *Fire Safety Journal,* vol. 88, pp. 96-103, 2017.

[21] G. J. Griffin, A. D. Bicknell, G. P. Bradbury and N. White, "Effect of Construction Method on the Fire Behavior of Sandwich Panels with Expanded Polystyrene Cores in Room Fire Tests," *Jornal of Fire Sciences,* vol. 24, no. 4, pp. 275-294, 2006.

[22] J. Axelsson and P. van Hees, "New Data for Sandwich Panels on the Correlation Between SBI Test Method and the Room Corner Reference Scenario," *Fire and Materials,* vol. 29, no. 1, pp. 53-59, 2004.

[23] V. Babrauskas, "Tables and Charts," in *Fire Protection Handbook, 17th edition,* Quincy MA, (A.E. Cote and J. Linville, eds.), NFPA, 1991.

[24] D. Cyganski, J. R. Duckworth and K. Notarianni, "Development of a Portable Flashover Predictor (Fire-Ground Environment Sensor System)," in *FEMA AFG 2008 Scientific Report,* Worchester Polytechnical Institute, 2010.